Ripple-Type Control for Enhancing Resilience of Networked Physical Systems

Manish K. Singh, Guido Cavraro, Andrey Bernstein, and Vassilis Kekatos

***Abstract*—Distributed control agents have been advocated as an effective means for improving the resiliency of our physical infrastructures under unexpected events. While purely local control has been shown to be insufficient, centralized optimal resource allocation approaches can be slow. In this context, we put forth a hybrid low-communication saturation-driven protocol for the coordination of control agents that are distributed over a physical system and are allowed to communicate with peers over a 'hotline' communication network. According to this protocol, agents act upon on local readings unless their control resources have been depleted, in which case they send a beacon for assistance to peer agents. Our ripple-type scheme triggers communication locally only for the agents with saturated resources, and is proved to converge. Moreover, under a monotonicity assumption on the underlying physical law coupling control outputs to inputs, the devised control is proved to converge to a configuration satisfying safe operational constraints. The assumption is shown to hold for voltage control in electric power systems and pressure control in water distribution networks. Numerical tests on both networks corroborate the efficacy of the novel scheme.**

***Index Terms*—Energy networks, event-triggered control, distributed control, resiliency, voltage control.**

I. Introduction

Utility systems, such as power, water, and gas networks, are significant examples of networked systems and are undergoing rapid changes. Power systems experience significant penetration of distributed energy resources and flexible load thus increasing the system volatility. Natural gas-fired generators serve as a fast-acting balancing mechanism for power systems, inadvertently increasing the volatility in gas networks. Rising threats of clean water scarcity have motivated tremendous efforts towards judicious planning for bulk water systems and enhanced monitoring and control for water distribution networks. Moreover, increasing occurrence of natural disasters and other critical (cyber and physical) disruptions undermines the stable and efficient operation of the aforesaid systems.

Classic operation of utility systems is performed via management systems that aim at satisfying consumer demands in a cost-effective manner while meeting the related operational and physical constraints. Such tasks constitute the family of optimal dispatch problems (ODP). ODPs are typically solved at regular intervals based on anticipated demands and network conditions. Stochastic optimization formulations are oftentimes leveraged to account for the uncertainty in network conditions and ensure reliable operation within the ODP interval. Although ODP solutions can ensure reliable system operation during normal conditions, they cannot account for the occurrence of low-probability high-impact disruptions that might undermine system operation. To improve system resilience to these events, emergency control schemes are required that can help avoid system collapse by executing fast actions in real time.

This paper focuses on the design of emergency control mechanisms that can ensure the satisfaction of system operational requirements during the time-interval between two ODP actions. The proposed strategy can be referred to as *ripple-type control* and draws features from local, distributed, and event-triggered control. In local control rules, agents take decision based upon on locally available readings. For example, in [1], [2], power generators control their reactive power output given their local power injection and voltage. However, local schemes have limited efficacy [3]. Distributed control strategies, in which agents compute their control action after sharing information with neighbors in a communication network, have a wide spectrum of applications, e.g., energy systems [4], [5], [6]; or camera networks [7]. To avoid wasting resources and communicate only when it is really needed, event-triggered control techniques have been advocated in [8], [9]. Essentially, every agent evaluates locally a *triggering function*, e.g., in a consensus setup, the mismatch between the current state and the state that was last sent to neighbors [10]. When the triggering function takes some specified values, agents communicate and update their control rule.

On the contrary, in the proposed ripple-type control, agents first try to satisfy their local constraints via purely local control. Only when such control efforts reach their maximum limit, an assistance is sought from neighboring agents on a communication graph. The process is continued until the control objectives of every agent are met. Another property of the proposed algorithm is that it is *model-free* in the sense that it does not require the knowledge of the system model parameters. This is an essential property of real-time emergency control due to lack of accurate model information during contingency scenarios [11].

A ripple-type control algorithm for ensuring satisfaction of operational requirements is devised and formally analyzed next. To show its applicability in real systems, the control scheme is tested on electric power and water networks.

Manish K. Singh and Vassilis Kekatos are with the Bradley Department of ECE, Virginia Tech, Blacksburg, VA 24061 USA (e-mail: {manishks, kekatos}@vt.edu). G. Cavraro and A. Bernstein are with the Power Systems Engineering Center, National Renewable Energy Laboratory, Golden, CO 80401 USA (e-mail: name.surname@nrel.gov). Work partially supported by the U.S. National Science Foundation under Grant 1711587. Manish K. Singh and Guido Cavraro contributed equally to this work.

II. System Modeling

Consider a networked system modeled [1] by an undirected graph $\mathcal{G} = (\mathcal{N}, \mathcal{E})$. The set $\mathcal{N}$ is a collection of N nodes hosting controllable agents and vector $\mathbf{x} \in \mathbb{R}^N$ represents their *control inputs*. A subset of agents comprising set $\mathcal{Y} \subset \mathcal{N}$ of cardinality M are assumed to be making local noiseless scalar observations, which are stacked in vector $\mathbf{y} \in \mathbb{R}^M$. The entries of $\mathbf{y}$, henceforth referred to as *outputs*, are to be regulated within a desired range. Given an input $\mathbf{x}$, the system has a locally unique output $\mathbf{y}$, determined by a mapping $\mathrm{F} : \mathbb{R}^N \to \mathbb{R}^M$. Heed that the mapping F may not necessarily have an explicit form. This work considers physical systems in which the related mapping F adheres to the following property.

Assumption 1. *The input-output mapping F is such that, for any* $\mathbf{x}$*,* $m \in \mathcal{Y}$*, and* $n \in \mathcal{N}$*, it holds*

$$\frac{\partial y_m}{\partial x_n} \geq 0$$

Albeit it might seem restrictive at the outset, the postulated monotonicity property holds true for several physical systems abiding by a dissipative flow law, such as natural gas transmission systems and water distribution networks; see e.g., [12]. Moreover, this assumption is approximately true for electric power systems as delineated next.

A. Electric Power Systems

This section considers the task of maintaining power transmission system voltages above given lower limits. A power transmission system may be modeled by a graph $\mathcal{G} = (\mathcal{N}, \mathcal{E})$, wherein electrical buses can be interpreted as agents. Buses in transmission networks are typically modeled as generator (PV) buses for which the active power injection and voltage magnitude are controlled; and load (PQ) buses for which the complex power injection is fixed and is independent of voltage. Let (v_n, q_n) denote the voltage magnitude (or simply voltage) and reactive power injection at bus $n \in \mathcal{N}$. Vectors $\mathbf{v}, \mathbf{q} \in \mathbb{R}^N$ collect the voltages and reactive injections across buses.

Transmission lines are often approximated as lossless, since their resistances are much smaller than their reactances. Thanks to this lossless approximation and the assumption of small voltage angle differences across neighboring buses, voltage angles (resp. magnitudes) are rather insensitive to variations in reactive (resp. active) power injections. To develop voltage control algorithms, the focus here is on the $\mathbf{q} - \mathbf{v}$ system . Vectors $\mathbf{v}$ and $\mathbf{q}$ adhere to the approximate model [13]

$$\mathbf{q} = \mathrm{dg}(\mathbf{v})\mathbf{B}\mathbf{v}. \tag{1}$$

where $\mathbf{B} \in \mathbb{R}^{N \times N}$ is a Laplacian matrix with line susceptances as weights. In detail, its (m, n)-th entry $B_{mn} < 0$ equals the negative susceptance of line $(m, n) \in \mathcal{E}$; it equals zero if there is no line between buses m and n; and its diagonal entries are $B_{mm} = -\sum_{n \neq m} B_{mn} > 0$.

Partition the node set $\mathcal{N}$ into generator and load buses as $\mathcal{N} = \mathcal{N}_S \oplus \mathcal{N}_L$. Arranging $\mathbf{v}$ and $\mathbf{q}$ as $\mathbf{v} = [\mathbf{v}_G^\top \ \mathbf{v}_L^\top]^\top$ and $\mathbf{q} = [\mathbf{q}_G^\top \ \mathbf{q}_L^\top]^\top$, model (1) can be written as

$$\begin{bmatrix} \mathbf{q}_G \\ \mathbf{q}_L \end{bmatrix} = \begin{bmatrix} \mathrm{dg}(\mathbf{v}_G) & \mathbf{0} \\ \mathbf{0} & \mathrm{dg}(\mathbf{v}_L) \end{bmatrix} \begin{bmatrix} \mathbf{B}_{GG} & \mathbf{B}_{GL} \\ \mathbf{B}_{LG} & \mathbf{B}_{LL} \end{bmatrix} \begin{bmatrix} \mathbf{v}_G \\ \mathbf{v}_L \end{bmatrix} \tag{2}$$

where $\mathbf{B}$ has been partitioned accordingly.

For the voltage regulation task at hand, the control variable depends on the type of each bus n:

$$x_n := \begin{cases} q_n & , \ n \in \mathcal{N}_L \\ v_n & , \ n \in \mathcal{N}_S \end{cases}.$$

Generators can control their voltages, while loads could partially control their reactive injections due to inverters, capacitor banks, and flexible AC transmission systems (FACTS).

By controlling the inputs $\mathbf{x}$, voltage regulation aims to maintain the load voltages $\mathbf{v}_L$ within acceptable levels. To this end, we need to analyze the dependence of the output $\mathbf{y} = \mathbf{v}_L$ on the control input $\mathbf{x} = [\mathbf{q}_L^\top \ \ \mathbf{v}_G^\top]^\top$. Unfortunately, the quadratic equations in (2) are not amenable to a closed-form expression of $\mathbf{y}$ in terms of $\mathbf{x}$. We thus adopt the linearization of [14] to compute the Jacobian matrix of $\mathbf{y}$ with respect to $\mathbf{x}$. Let $\tilde{v} := \min_{n \in \mathcal{N}_G} v_n$ and define

$$\begin{bmatrix} \boldsymbol{\epsilon}_G \\ \boldsymbol{\epsilon}_L \end{bmatrix} := \frac{1}{\tilde{v}} \begin{bmatrix} \mathbf{v}_G \\ \mathbf{v}_L \end{bmatrix} - \mathbf{1}. \tag{3}$$

The second block equation of (2) provides

$$\begin{aligned} \mathbf{q}_L &= \tilde{v}^2 \, \mathrm{dg}(\mathbf{1} + \boldsymbol{\epsilon}_L) \left(\mathbf{B}_{LG}(\mathbf{1} + \boldsymbol{\epsilon}_G) + \mathbf{B}_{LL}(\mathbf{1} + \boldsymbol{\epsilon}_L) \right) \\ &\simeq \tilde{v}^2 (\mathbf{B}_{LG}\boldsymbol{\epsilon}_G + \mathbf{B}_{LL}\boldsymbol{\epsilon}_L), \end{aligned} \tag{4}$$

wherein we ignored terms involving products between ϵ's and used the property $[\mathbf{B}_{LG} \ \mathbf{B}_{LL}]\mathbf{1} = \mathbf{0}$ of $\mathbf{B}$. Solving for $\boldsymbol{\epsilon}_L$ in (4) and re-substituting voltages from (3) yields

$$\mathbf{v}_L \simeq \frac{1}{\tilde{v}} \mathbf{B}_{LL}^{-1} \mathbf{q}_L - \mathbf{B}_{LL}^{-1} \mathbf{B}_{LG} \mathbf{v}_G. \tag{5}$$

Equation (5) approximates the mapping F for the voltage regulation task. Being a diagonal block of a Laplacian, matrix $\mathbf{B}_{LL}$ is known to be positive definite and hence a non-singular; see e.g., [15]. Because in addition its off-diagonal entries are non-positive, matrix $\mathbf{B}_{LL}$ is an M-matrix, so that all entries of $\mathbf{B}_{LL}^{-1}$ are non-negative. This establishes that the Jacobian of $\mathbf{y} = \mathbf{v}_L$ with respect to $\mathbf{q}_L$ has non-negative entries. The same property holds for the Jacobian of $\mathbf{v}_L$ with respect to $\mathbf{v}_G$ since $\mathbf{B}_{LG}$ has non-positive entries. The previous arguments show that the approximate model (1) satisfies Assumption 1. This linearized model is employed due to analytical convenience for verifying Assumption 1. However, the numerical tests in Section V use a nonlinear AC power flow model [16].

B. Water Distribution Networks

A water distribution system (WDS) can be modeled by an undirected graph $\mathcal{G} = (\mathcal{N}, \mathcal{E})$, where the nodes in $\mathcal{N}$ correspond to water reservoirs, tanks, junctions and consumers. If d_n denotes the rate of water injection at node n, then $d_n \geq 0$ for reservoirs; $d_n \leq 0$ for water consumers; tanks may be

[1] *Notation*: Lower- (upper-) case boldface letters denote column vectors (matrices). Sets are represented by calligraphic symbols. Symbol $^\top$ stands for transposition. Inequalities, max, and min operators are understood elementwise. All-zero and all-one vectors are represented by $\mathbf{0}$ and $\mathbf{1}$; the respective dimensions are deducible from context. The $\mathrm{dg}(\cdot)$ operator on vectors places the vector on the principal diagonal of a matrix; for argument being a matrix, it extracts the diagonal as a vector. Symbol $\|\cdot\|$ represents the L_2 norm.

filling or emptying; and $d_n = 0$ for junctions. Nodes are connected by edges in $\mathcal{E}$ which represent pipelines, pumps and valves. Let σ_{mn} denote the water flow rate on edge (m, n) along the direction from m to n, with $\sigma_{mn} = -\sigma_{nm}$. Flow conservation at node n dictates

$$d_n = \sum_{m:(n,m)\in\mathcal{E}} \sigma_{nm}. \tag{6}$$

The relation between water flow σ_{mn} across edge (m, n) and the pressures π_m and π_n at nodes m and n takes the form

$$\pi_m - \pi_n = \rho_{mn}(\sigma_{mn}). \tag{7}$$

The operation of a WDS involves serving water demands while maintaining nodal pressures within desirable levels. The task of pressure control may include continuous-valued variables, such as reservoir and tank output pressures, as well as water injections at different nodes. Pressure control may also involve binary variables capturing the on/off status of fixed-speed pumps and valves [17]. These continuous and binary control variables are oftentimes determined by periodically solving ODPs; see [17] and references therein. Assuming the binary variables to be fixed between two ODP instances, we next focus on the continuous-valued variables. Partition set $\mathcal{N}$ into the subset $\mathcal{N}_S$ comprising of reservoirs and tanks, and subset $\mathcal{N}_L$ representing loads. The pressures and demands for nodes in $\mathcal{N}_S$ and $\mathcal{N}_L$, respectively, are assumed to be controllable. This is without loss of generality as inelastic quantities can be modeled with lower and upper limits coinciding. Thus, the control variables are

$$x_n := \begin{cases} \pi_n & , \ n \in \mathcal{N}_S \\ d_n & , \ n \in \mathcal{N}_L \end{cases}.$$

Given $\mathbf{x}$, the water injections for the nodes in $\mathcal{N}_S$ and the pressures at nodes in $\mathcal{N}_L$ are determined by the water flow equations (6)–(7). Since nodal pressures over $\mathcal{N}_L$ need to be maintained at stipulated levels, they constitute vector $\mathbf{y}$. Note that for the aforementioned assignments of vectors $\mathbf{x}$ and $\mathbf{y}$, the mapping F is implicitly defined by (6)–(7). Reference [18] guarantees that the mapping F maps a given $\mathbf{x}$ to a unique $\mathbf{y}$.

To verify the validity of Assumption 1, we will use a monotonicity result for dissipative flow networks from [12]. To qualify as a disspative flow network per [12], functions $\rho_{mn}(\cdot)$ should be non-decreasing and continuous. Both these requirements hold true for edges in a WDS. Specifically, for a pipe $(m, n) \in \mathcal{E}$, the function ρ_{mn} models the pressure drop due to friction along the pipe described by the Darcy-Weisbach or the Hazen-Williams laws [18]; both being non-decreasing and continuous. For pumps and valves, pressures π_m and π_n relate to flow σ_{mn} via non-decreasing empirical laws as well [19]. Therefore, WDS come within the purview of dissipative networks and the ensuing result applies [12].

Lemma 1. *[12, Corollary 4] Let $\boldsymbol{\pi}$ and $\boldsymbol{\pi}'$ be N-length pressure vectors satisfying the water flow equations* (6)-(7) *for demand vectors $\mathbf{d}$ and $\mathbf{d}'$. If $\pi_n \geq \pi'_n$ for all $n \in \mathcal{N}_S$, and $d_n \geq d'_n$ for all $n \in \mathcal{N}_L$, then $\pi_n \geq \pi'_n$ for all $n \in \mathcal{N}_L$.*

In terms of the assigned vectors $\mathbf{x}$ and $\mathbf{y}$, Lemma 1 states that controls $\mathbf{x} \geq \mathbf{x}'$ result in $\mathbf{y} \geq \mathbf{y}'$. Thus, considering infinitesimal changes at node pairs m and n, Lemma 1 translates to $\frac{\partial y_m}{\partial y_n} \geq 0$, hence satisfying Assumption 1.

III. Problem Formulation

Operators manage the networked system by computing periodically the control setpoints that agents should implement. Usually, these control setpoints are the solution of an *optimal dispatch problem* (ODP) of the form

$$\begin{aligned} \mathbf{x}^* \in \arg\min_{\mathbf{x}} \quad & c(\mathbf{x}, \mathbf{y}) && \text{(ODP)} \\ \text{s.to} \quad & \mathbf{y} = \mathrm{F}(\mathbf{x}) && \text{(8a)} \\ & \mathbf{h}(\mathbf{x}, \mathbf{y}) \leq 0, && \text{(8b)} \\ & \underline{\mathbf{x}} \leq \mathbf{x} \leq \bar{\mathbf{x}} && \text{(8c)} \\ & \mathbf{y} \geq \underline{\mathbf{y}} && \text{(8d)} \end{aligned}$$

where $c(\mathbf{x}, \mathbf{y})$ is a cost function depending on both the system inputs and outputs; the mapping in (8a) corresponds to the physical laws governing the networked system; while inequality constraints can be divided into two categories:

- The function in (8b) captures requirements that are important for efficiently operating the system, but can in principle be safely violated (especially for a short amount of time). These will be referred to as *soft constraints*.
- Constraints (8c) and (8d) impose limitations on input and output variables, respectively. If violated, they can lead to system failure. These constraints will be referred to as *hard constraints*.

Typically, given the set of parameters defining mapping F, a central dispatcher solves (ODP) and communicates optimal control setpoints $\mathbf{x}^*$ to agents. Ideally, this process shall be repeated every time there is a change in the system model that modifies the underlying definition of F, such as an abrupt load change or line tripping for the case of power systems. Constrained by communication and computational resources however, problem (ODP) is solved only at finite time intervals. As a consequence, the setpoints $\mathbf{x}^*$ can become obsolete or even result in network constraint violations.

Such limitations motivate the design of mechanisms to at least ensure that some important operational requirements are met between two consecutive centralized dispatch actions, i.e., to make the control vector $\mathbf{x}$ belong to the feasible set

$$\mathcal{F} = \{\mathbf{x} : \ \underline{\mathbf{x}} \leq \mathbf{x} \leq \bar{\mathbf{x}}, \ \mathbf{y} = \mathrm{F}'(\mathbf{x}), \mathbf{y} \geq \underline{\mathbf{y}}\}$$

in which F' is the input-output mapping defined by the system model after a disruptive event. Set $\mathcal{F}$ only considers the hard constraints of (ODP), namely (8c) and (8d).

Remark 1. *For power systems, constraint* (8b) *models line flow limits, which can be considered soft constraints as their violation could be briefly tolerated. Limits on the power or voltage output of generators are captured by* (8c)*. Inequality* (8d) *models load voltage constraints. Avoiding dangerously low voltages is important to prevent a voltage collapse.*

Remark 2. *For water distribution systems, the inequalities* (8b) *can represent the water flow limits on pipes and pumps. Although such limits shall normally be respected, they can be characterised as soft over short time intervals.*

Constraints (8c) *represent the limits on pressure at water sources and demands by consumers. These limits can not be violated physically as they are determined by the actual capacity of the WDS components and available demands. The inequalities in* (8d) *can model the minimum pressure requirements at consumer nodes. The latter requirements must be adhered to at all times as low pressures may cause service failures and equipment malfunction at the consumer end.*

IV. Ripple-Type Network Control

We next put forth an algorithm for steering $\mathbf{x}$ to $\mathcal{F}$ with the ensuing key attributes:

- *A1)* Agent $n \in \mathcal{Y}$ measures y_n and controls x_n locally. Upon a violation of (8d), local control resources are used first.
- *A2)* Agent n transmits communication signals to a few peer agents over a "hotline" communication network only if $x_n = \bar{x}_n$, i.e., only when local control resources reach their maximum limit, assistance is sought from neighboring nodes on a communication graph; and
- *A3)* The control scheme is agnostic to system parameters, i.e., it is a model-free approach that does not require explicit knowledge of operator F'.

The hotline communication network is modeled as a graph $\mathcal{G}_c = (\mathcal{N}, \mathcal{E}_c)$ in which the communication links $\mathcal{E}_c$ do not necessarily coincide with the physical connections among agents. Graph $\mathcal{G}_c$ is henceforth assumed to be connected. Considering unit edge weights for $\mathcal{G}_c$, we denote its Laplacian matrix as $\mathbf{L}_c$. Setting the diagonals of the Laplacian matrix to zero, define $\mathbf{L} := \mathbf{L}_c - \mathrm{dg}(\mathrm{dg}(\mathbf{L}_c))$. Let us also introduce function $\mathbf{f} : \mathbb{R}^N \to \mathbb{R}^N$ defined entry-wise as

$$f_n(\mathbf{x}) := \begin{cases} \underline{y}_n - y_n(\mathbf{x}), & \underline{y}_n \geq y_n(\mathbf{x}), n \in \mathcal{Y} \\ 0, & \text{otherwise.} \end{cases} \tag{9}$$

Assume that, at time $t = 0$, a violation of (8d) occurs as a consequence of a model change. Let $\mathbf{x}(0)$ be the initial control variables, and introduce an auxiliary vector $\boldsymbol{\lambda} \in \mathbb{R}^N$, which is initialized as $\boldsymbol{\lambda}(0) = \mathbf{0}$. At subsequent times $t \geq 1$, the control scheme proceeds in four steps as delineated next.

Step 1: Agents compute $\mathbf{f}(\mathbf{x}(t)) \geq \mathbf{0}$ according to (9). The entries of $\mathbf{f}(\mathbf{x}(t))$ are strictly positive if the associated nodes in $\mathcal{Y}$ experience a violation of (8d); and zero, otherwise.

Step 2: A target setpoint is computed as

$$\hat{\mathbf{x}}(t+1) = \mathbf{x}(t) + \mathrm{dg}(\boldsymbol{\eta}_1)\mathbf{f}(\mathbf{x}(t)) - \mathrm{dg}(\boldsymbol{\eta}_2)\mathbf{L}\boldsymbol{\lambda}(t) \tag{10}$$

for positive $\boldsymbol{\eta}_1$ and $\boldsymbol{\eta}_2$. Note that for node n, the target $\hat{x}_n(t)$ is computed using the local reading $y_n(t)$ and the entries of $\boldsymbol{\lambda}$ sent from its peers (neighbor nodes of node n on $\mathcal{G}_c$).

Step 3: Agents compute the auxiliary vector $\boldsymbol{\lambda}$ as

$$\boldsymbol{\lambda}(t+1) = \max\{\mathbf{0}, \mathrm{dg}(\boldsymbol{\eta}_3)(\hat{\mathbf{x}}(t+1) - \bar{\mathbf{x}})\}. \tag{11}$$

for a positive $\boldsymbol{\eta}_3$. Vector $\boldsymbol{\lambda}$ serves as a beacon for assistance that is communicated across peer nodes.

Step 4: The target setpoint is projected to the feasible range

$$\mathbf{x}(t+1) = \min\{\hat{\mathbf{x}}(t+1), \bar{\mathbf{x}}\}, \tag{12}$$

and is physically implemented.

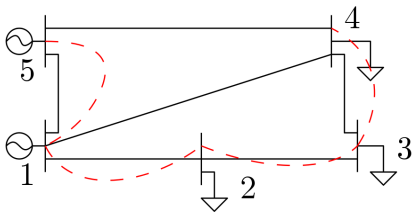

Fig. 1. Modified PJM system. Communication links as red dashed lines.

To establish the effectiveness, Proposition 1 proves that the proposed scheme reaches an equilibrium point and Proposition 2 that this equilibrium belongs to $\mathcal{F}$. The proofs for these results are provided in the Appendix.

Proposition 1. *Given any* $\mathbf{x}(0)$*, the sequence* $\{\mathbf{x}(t)\}$ *converges asymptotically.*

Proposition 2. *Let Assumption 1 hold,* $\mathcal{F}$ *be non-empty, and*

$$\|\mathrm{dg}(\boldsymbol{\eta}_2)\,\mathrm{dg}(\boldsymbol{\eta}_3)\mathbf{L}\| < 1. \tag{13}$$

A pair $(\mathbf{x},\ \boldsymbol{\lambda})$ *is an equilibrium for the proposed scheme if and only if* $\mathbf{x}$ *belongs to* $\mathcal{F}$ *and* $\boldsymbol{\lambda} = \mathbf{0}$.

The novel control scheme satisfies attribute *A1)* by design. Moreover, for a node n with target setpoints $\hat{x}_n(t+1)$ within the local control limit $\bar{x}_n$, the corresponding entry of $\boldsymbol{\lambda}(t+1)$ is zero. Thus the computation of $\hat{x}_m$ from (10) for nodes m that are neighbors of n requires no communication from node n, hence fulfilling *A2)*. The scheme also meets *A3)* since it is agnostic to changes in topology and/or demands.

Remark 3. *Apparently, parameter* $\boldsymbol{\eta}_1$ *does not influence the control scheme convergence. Indeed,* (13) *provides a condition only on* $\boldsymbol{\eta}_2$ *and* $\boldsymbol{\eta}_3$*. However,* $\boldsymbol{\eta}_1$ *plays a role in determining the equilibrium point and the speed of convergence, whose analytical quantification is beyond the scope of this work.*

V. Numerical Tests

The control algorithm was tested for two utility network applications: voltage control in power systems and pressure control in water systems. Commencing with the power system, parameters $\boldsymbol{\eta}_2$ and $\boldsymbol{\eta}_3$ were chosen so that (13) holds true.

A. A Power System Test Case

The benchmark network used for the tests on power systems is a modified version of the PJM 5-bus system [20] shown in Fig. 1. Buses 1 and 2 serve as generators, whereas buses 3, 4, and 5 are loads. Generators are allowed to raise their voltage output to 1.02 p.u.; loads can reduce their power demand by 10 MW and their voltages are required to be above $V_{thr} = 0.94$ p.u., which represents a safe threshold. The top panel of Figure 2 shows the bus voltage trajectories, while the bottom panel plots the ratio of control resources used $x_n/\bar{x}_n$. After an abnormal event, buses 2 and 3 find themselves with voltage below V_{thr} and start performing the proposed control strategy. Since their local efforts do not manage to regulate the voltages, they seek assistance from their neighbors in the communication network, precisely, bus 4 (around the 200-th

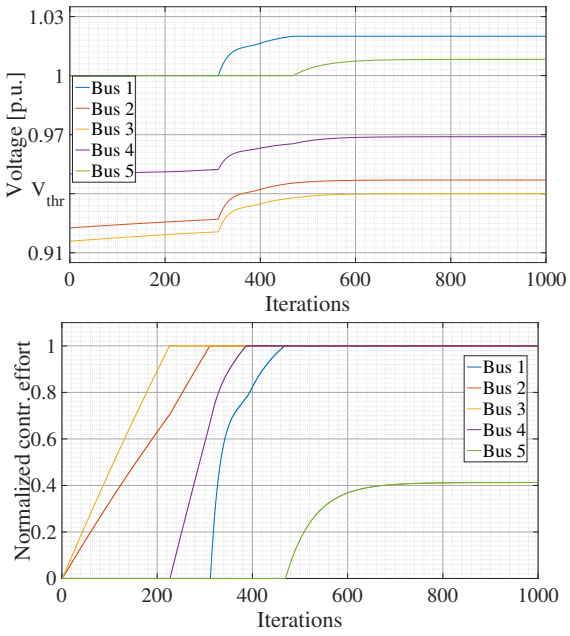

Fig. 2. *Top:* Bus voltages. *Bottom:* Normalized control effort $x_n/\bar{x}_n$ used.

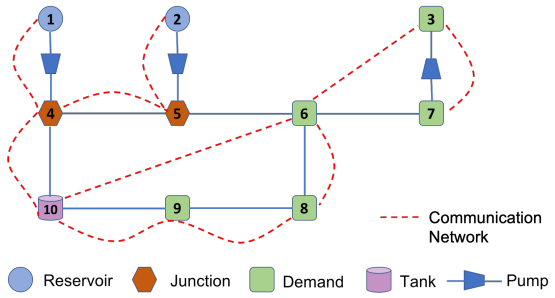

Fig. 3. A 10-node benchmark water distribution system.

iteration) and bus 1 (around the 300-th iteration). Finally, when bus 1 hits its control limits, bus 5 kicks in (after the 400-th iteration) and is finally able to bring the voltage within the safe interval.

B. A Water Network Test Case

The proposed algorithm was applied for pressure task on the 10-node WDS of Fig. 3, which consists of 2 reservoirs and a tank; 3 fixed-speed pumps; and 7 lossy pipes. Pipe dimensions and friction coefficients were taken from [17]. The minimum pressure requirement $\underline{\pi}_n$ for nodes 3 to 10 is $\{10, 7, 10, 10, 5, 10, 10, 10\}$ m. The pumps $(1, 2)$, $(2, 5)$, and $(7, 3)$ are considered to be operating at fixed speeds with constant pressure gains of 10, 10, and 5 m, respectively. All water flow instances were solved using the optimization-based solver of [18]. The base operating condition involves injection $\mathbf{d}_0 = [380, 300, -170, 0, 0, -220, -200, -150, -140, 200]^\top \text{m}^3/\text{hr}$ and $\boldsymbol{\pi} = [3.0, 1.8, 11.6, 13, 11.9, 10.2, 6.6, 10.3, 10.9, 12.9]^\top$m. A disruption was modeled by considering a failure of pump $(2, 5)$ resulting in unavailability of node 2 reservoir and reservoir at node 1 supplying

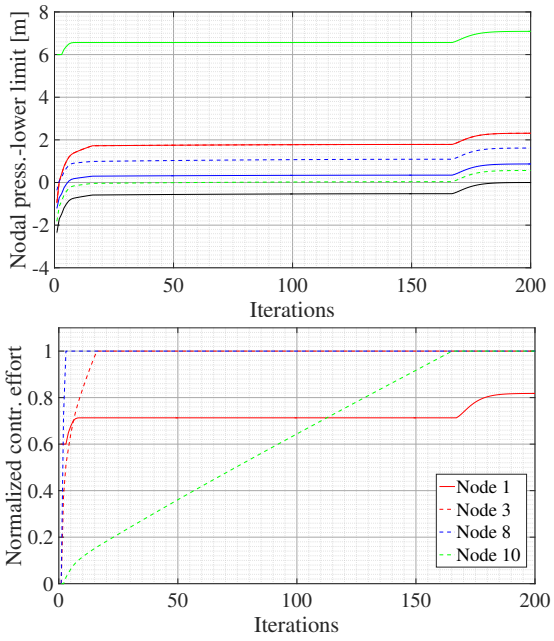

Fig. 4. *Top:* Difference of pressures at nodes 3-10 from their lower limits. *Bottom:* Normalized control effort $x_n/\bar{x}_n$ used at nodes 1, 3, 8, and 10

$d_1 = 680\text{m}^3/\text{hr}$. This contingency would result in $\boldsymbol{\pi} = [3.0, 0, 9.1, 13, 8.8, 7.7, 4.1, 8.2, 9.6, 12.7]^\top$ m, which violates the minimum pressure needed at nodes 3 and $5 - 9$.

To study a scenario where not all agents have control capability, only two demand nodes, namely 3 and 8, are allowed to reduce demand by 50 m^3/hr. Further, the tank node 10 has an injection flexibility of ± 200 m^3/hr and reservoir 1 has a controllable pressure range of $[0, 5]$ m. The performance of the proposed algorithm in restoring the pressures is demonstrated in Fig. 4. The top panel shows the difference $\pi_n - \underline{\pi}_n$ for nodes $n = \{3 \dots 10\}$. As anticipated, the pressures are non-decreasing and the algorithm succeeds in restoring them above the respective lower limits. The bottom panel plots the ratio of control resource used $x_n/\bar{x}_n$ for nodes $\{1, 3, 8, 10\}$. As desired, once all pressures are restored at desired levels, the algorithm attains an equilibrium and $\mathbf{x}$ saturates.

VI. Conclusions

A novel ripple-type coordination scheme for emergency control of networked systems has been put forth. The involved agents act based upon local control rules as long as local resources have not been saturated. Otherwise, they solicit help from peer agents through a "hotline" communication network not necessarily coinciding with the underlying physical system graph. The algorithm provably converges to safe operating conditions under an appropriate choice of parameters. Its validity has been illustrated on power and water network examples.

Appendix

Proof of Proposition 1: Owing to the projection in (12), it is evident that $\mathbf{x}(t) \leq \bar{\mathbf{x}}$ for all t. Thus, proving a non-decreasing property $\mathbf{x}(t) \leq \mathbf{x}(t+1)$ for all t is sufficient for

establishing convergence of the sequence $\{\mathbf{x}(t)\}$. Consider an arbitrary node n and time t. When $x_n(t+1) = \bar{x}_n$ we trivially have $x_n(t) \leq x_n(t+1)$. When $x_n(t+1) < \bar{x}_n$, *Step 4* yields $\hat{x}_n(t+1) = x_n(t+1)$ and (10) implies

$$x_n(t+1) = x_n(t) + \eta_{1,n} f_n(t) - \eta_{2,n} \sum_{m=1}^{N} L_{nm} \lambda_m(t) \geq x_n(t)$$

because $f_n(t)$ and $\boldsymbol{\lambda}_m(t)$ are non-negative; $\eta_{1,n}$ and $\eta_{2,n}$ are positive; and matrix $\mathbf{L}$ has non-positive entries. ■

Proof of Proposition 2: Assume $\mathbf{x} \in \mathcal{F}$ and $\boldsymbol{\lambda} = \mathbf{0}$. It follows that $\mathbf{y}(\mathbf{x}) \geq \underline{\mathbf{y}}$ and so $\mathbf{f}(\mathbf{x}) = \mathbf{0}$ from (9). Upon initializing the proposed control scheme at $\mathbf{x}$ and $\boldsymbol{\lambda}$, *Step 1* provides $\mathbf{f}(\mathbf{x}) = \mathbf{0}$; *Step 2* yields $\hat{\mathbf{x}}(1) = \mathbf{x}$; *Step 3* provides $\boldsymbol{\lambda}(1) = \mathbf{0}$; and *Step 4* that $\mathbf{x}(1) = \mathbf{x}$. Therefore, $(\mathbf{x},\ \boldsymbol{\lambda})$ is an equilibrium for the proposed control steps.

To establish the reverse direction, we will prove the contrapositive statement, i.e., if $\mathbf{x}$ does not belong to $\mathcal{F}$ or $\boldsymbol{\lambda} \neq \mathbf{0}$, then $(\mathbf{x}, \boldsymbol{\lambda})$ is not an equilibrium. We show the two cases separately using proof by contradiction.

Case 1) Vector $\mathbf{x}$ does not belong to $\mathcal{F}$: Since $\mathcal{F}$ is not empty by hypothesis, Assumption 1 implies that $\mathbf{y}(\bar{\mathbf{x}}) \geq \mathbf{y}(\mathbf{x}')$ for $\underline{\mathbf{x}} \leq \mathbf{x}' \leq \bar{\mathbf{x}}$ and hence

$$\mathbf{y}(\bar{\mathbf{x}}) \geq \underline{\mathbf{y}}. \tag{14}$$

In other words, applying the maximum control effort makes the constraints on observed outputs hold. Suppose $\mathbf{x} \notin \mathcal{F}$, yet there exists a $\boldsymbol{\lambda}$ such that $(\mathbf{x}, \boldsymbol{\lambda})$ is an equilibrium for the algorithm. Since $\mathbf{x}$ is projected in its permissible range by (12), its infeasibility means there exists a node $n \in \mathcal{Y}$ such that

$$\underline{y}_n > y_n(\mathbf{x}). \tag{15}$$

Define $\hat{x}_n := x_n + \eta_{1,n} f_n(\mathbf{x}) - \eta_{2,n} \sum_{\ell=1}^{N} L_{n,\ell} \lambda_\ell$ as in (10). Because $f_n(\mathbf{x}) > 0$, it follows that $\hat{x}_n > x_n$. However, since by hypothesis $x_n = \min\{\hat{x}_n, \bar{x}_n\}$, it follows that $x_n = \bar{x}_n$ and $\hat{x}_n > \bar{x}_n$, so that $\lambda_n > 0$.

Consider a node m neighbor of n in $\mathcal{G}_c$ and define

$$\hat{x}_m = x_m + \eta_{1,m} f_m(\mathbf{x}) - \eta_{2,m} \sum_{\ell=1}^{N} L_{m,\ell} \lambda_\ell. \tag{16}$$

Since $\lambda_n > 0$ and $x_m = \min\{\hat{x}_m, \bar{x}_m\}$, it holds again that $\hat{x}_m > x_m = \bar{x}_m$ and so $\lambda_m > 0$. Repeating this argument for all neighbors of n, one gets that $\boldsymbol{\lambda} > \mathbf{0}$ and that

$$\mathbf{x} = \bar{\mathbf{x}}. \tag{17}$$

This concludes the proof for Case 1 since (15) and (17) contradict (14).

Case 2) Vector $\boldsymbol{\lambda} \neq \mathbf{0}$: Suppose $\mathbf{x} \in \mathcal{F}$, and there exists a $\boldsymbol{\lambda} \neq \mathbf{0}$ such that $(\mathbf{x}, \boldsymbol{\lambda})$ is an equilibrium for the proposed scheme. First, note that by plugging (10) into (11), we can express $\boldsymbol{\lambda}(t+1)$ as a function of $\boldsymbol{\lambda}(t)$ and $\mathbf{x}(t)$ as

$$\boldsymbol{\lambda}(t+1) = \max\big\{\mathbf{0}, \operatorname{dg}(\boldsymbol{\eta}_3)\big(\mathbf{x}(t) + \operatorname{dg}(\boldsymbol{\eta}_1)\mathbf{f}(\mathbf{x}(t)) - \operatorname{dg}(\boldsymbol{\eta}_2)\mathbf{L}\boldsymbol{\lambda}(t) - \bar{\mathbf{x}}\big)\big\}.$$

The feasibility assumption provides $\mathbf{f}(\mathbf{x}) = \mathbf{0}$ and the equilibrium condition yields

$$\begin{aligned}\boldsymbol{\lambda} &= \max\big\{\mathbf{0}, \operatorname{dg}(\boldsymbol{\eta}_3)\big(\mathbf{x} - \operatorname{dg}(\boldsymbol{\eta}_2)\mathbf{L}\boldsymbol{\lambda} - \bar{\mathbf{x}}\big)\big\} \\ &\leq \max\big\{\mathbf{0}, -\operatorname{dg}(\boldsymbol{\eta}_3)\operatorname{dg}(\boldsymbol{\eta}_2)\mathbf{L}\boldsymbol{\lambda}\big\} \\ &\leq -\operatorname{dg}(\boldsymbol{\eta}_3)\operatorname{dg}(\boldsymbol{\eta}_2)\mathbf{L}\boldsymbol{\lambda} \end{aligned} \tag{18}$$

where the first and the second inequalities stem from the fact that $\mathbf{x} - \bar{\mathbf{x}}$ and $\operatorname{dg}(\boldsymbol{\eta}_2)\operatorname{dg}(\boldsymbol{\eta}_3)\mathbf{L}\boldsymbol{\lambda}(t)$ have non-positive entries.

Invoking the norm inequality on (18), we get $\|\boldsymbol{\lambda}\| \leq \|\operatorname{dg}(\boldsymbol{\eta}_2)\operatorname{dg}(\boldsymbol{\eta}_3)\mathbf{L}\|\|\boldsymbol{\lambda}\|$. Also, using the condition $\|\operatorname{dg}(\boldsymbol{\eta}_2)\operatorname{dg}(\boldsymbol{\eta}_3)\mathbf{L}\| < 1$ with $\boldsymbol{\lambda} \neq \mathbf{0}$ yields $\|\boldsymbol{\lambda}\| < \|\boldsymbol{\lambda}\|$, which is a contradiction. ■

REFERENCES

[1] H. Zhu and H. J. Liu, "Fast local voltage control under limited reactive power: Optimality and stability analysis," *IEEE Trans. Power Syst.*, vol. 31, no. 5, pp. 3794–3803, Sep. 2016.

[2] X. Zhou, M. Farivar, Z. Liu, L. Chen, and S. Low, "Reverse and forward engineering of local voltage control in distribution networks," *IEEE Trans. Autom. Contr.*, pp. 1–1, May 2020.

[3] S. Bolognani, R. Carli, G. Cavraro, and S. Zampieri, "On the need for communication for voltage regulation of power distribution grids," *IEEE Trans. Control Netw. Syst.*, vol. 6, no. 3, pp. 1111–1123, Sep. 2019.

[4] G. Cavraro and R. Carli, "Local and distributed voltage control algorithms in distribution networks," *IEEE Trans. Power Syst.*, vol. 33, no. 2, pp. 1420–1430, March 2018.

[5] A. Bernstein and E. Dall'Anese, "Real-time feedback-based optimization of distribution grids: A unified approach," *IEEE Trans. Control Netw. Syst.*, vol. 6, no. 3, pp. 1197–1209, Sep. 2019.

[6] C. Chang, M. Colombino, J. Corté, and E. Dall'Anese, "Saddle-flow dynamics for distributed feedback-based optimization," *IEEE Contr. Syst. Lett.*, vol. 3, no. 4, pp. 948–953, Oct. 2019.

[7] N. Bof, R. Carli, A. Cenedese, and L. Schenato, "Asynchronous distributed camera network patrolling under unreliable communication," *IEEE Trans. Autom. Contr.*, vol. 62, no. 11, pp. 5982–5989, Nov. 2017.

[8] W. P. M. H. Heemels, K. H. Johansson, and P. Tabuada, "An introduction to event-triggered and self-triggered control," in *Proc. IEEE Conf. on Decision and Control*, Maui, HI, Dec. 2012, pp. 3270–3285.

[9] S. Magnusson, C. Fischione, and N. Li, "Optimal voltage control using event triggered communication," in *Proc. 10th ACM Int. Conf. Future Energy Syst. (e-Energy)*, Phoenix, AZ, Jun. 2019, pp. 343–354.

[10] C. Nowzari and J. Cortés, "Distributed event-triggered coordination for average consensus on weight-balanced digraphs," *Automatica*, vol. 68, pp. 237–244, Jun. 2016.

[11] Y. Chen, A. Bernstein, A. Devraj, and S. Meyn, "Model-free primal-dual methods for network optimization with application to real-time optimal power flow," in *Proc. American Control Conf.*, Denver, CO, Jul. 2020, pp. 3140–3147.

[12] M. Vuffray, S. Misra, and M. Chertkov, "Monotonicity of dissipative flow networks renders robust maximum profit problem tractable: General analysis and application to natural gas flows," in *Proc. IEEE Conf. on Decision and Control*, Osaka, Japan, Dec. 2015, pp. 4571–4578.

[13] J. W. Simpson-Porco, F. Dorfler, and F. Bullo, "Voltage stabilization in microgrids via quadratic droop control," *IEEE Trans. Autom. Contr.*, vol. 62, no. 3, pp. 1239–1253, Mar. 2017.

[14] B. Gentile, J. Simpson-Porco, F. Dorfler, S. Zampieri, and F. Bullo, "On reactive power flow and voltage stability in microgrids," in *Proc. American Control Conf.*, Portland, OR, Jun. 2014, pp. 759–764.

[15] A. M. Kettner and M. Paolone, "On the properties of the power systems nodal admittance matrix," *IEEE Trans. Power Syst.*, vol. 34, no. 1, pp. 444–453, Jan. 2019.

[16] R. D. Zimmerman, C. E. Murillo-Sanchez, and R. J. Thomas, "MATPOWER: steady-state operations, planning and analysis tools for power systems research and education," *IEEE Trans. Power Syst.*, vol. 26, no. 1, pp. 12–19, Feb. 2011.

[17] M. K. Singh and V. Kekatos, "Optimal scheduling of water distribution systems," *IEEE Trans. Control Netw. Syst.*, vol. 7, no. 2, pp. 711–723, Jun. 2020.

[18] ——, "On the flow problem in water distribution networks: Uniqueness and solvers," Feb. 2019, (under review). [Online]. Available: https://arxiv.org/abs/1901.03676

[19] D. Cohen, U. Shamir, and G. Sinai, "Optimal operation of multi-quality water supply systems-II: The Q-H model," *Engineering Optimization*, vol. 32, no. 6, pp. 687–719, Oct. 2000.

[20] F. Li and R. Bo, "Small test systems for power system economic studies," in *Proc. IEEE Power & Energy Society General Meeting*, Providence, RI, Jul. 2010, pp. 1–4.